JOURNAL OF MATERIALS SCIENCE 31 (1996) 581–587

Change in the type of majority carriers in disordered In_xSe_{100-x} thin-film alloys

S. MARSILLAC, J. C. BERNÈDE, A. CONAN
Laboratoire de Physique des Matériaux pour l'Electronique, Faculté des Sciences et des Techniques de Nantes, 2 rue de la Houssinière, 44072 Nantes cédex 03, France

Electrical, optical and physico-chemical properties of disordered In_xSe_{100-x} thin films have been investigated for x ranging from 40–65. The films are found to be p-type for composition ranging from 45–60 at% selenium and n-type for compositions below 40 at% selenium. An increase in the conductivity, together with a decrease of the activation energy and of the optical gap, has also been observed when x varies from 40–65. These results have been interpreted through a theory based on the relative percentage evolution of the In–In and Se–Se chemical bonds and, on the other hand, by a percolation theory due to microcrystalline structures and indium filaments. These two models are discussed in reference to other publications.

1. Introduction

In recent years, polycrystalline and amorphous indium selenide (InSe) thin films have attracted attention as a new material for applications as solar cells [1–6], for memory applications (switching) [7, 8] and other devices [9, 10]. While usually amorphous chalcogenides films show p-type conductivity [11], a very large diversity of results about the n or p character of InSe thin films can be found in previous works, even for similar composition. "Amorphous" thin films are found to be n-type [7, 12, 13] or p-type [14–16]. Available results are sometimes hard to find, because the determination of carrier type is not usually the main result of the work, it is only a complement. Furthermore, as the layers are not systematically characterized, some measurements may not have been made (microprobe and XPS analyses after deposition, TEM measurements for structural analysis).

It is important to notice that for films such as InSe with multiphase crystalline possibilities, the starting material, the preparation and deposition techniques are very important [12]. However, these results have not been much discussed. In this work, we studied the properties of amorphous In_xSe_{100-x} layers. It was found that, at room temperature, the sign of the carriers depends on the selenium atomic concentration. This new result could be interesting for some device applications.

2. Experimental techniques

The starting material was prepared by mixing quantities of high purity (99.999%) indium and selenium pellets in various calculated ratios. The mixture was sealed in an evacuated Pyrex tube and heated at 823 K for 24 h. In_xSe_{100-x} thin films were obtained by classical thermal evaporation of the powder from a molybdenum boat, under a vacuum better than 10^{-4} Pa. A shutter was used at the beginning and at the end of the heating of the boat, to avoid contamination of the substrate. The evaporation boat has a special configuration (two superposed multiholed covers) in order to avoid the calefaction of the In_xSe_{100-x} powder. The substrates were glass, NaCl freshly cleaved crystal for TEM measurement or stainless steel slides, for X-ray photoelectron spectroscopy (XPS) anlaysis. The evaporation rate (1–1.5 nm s^{-1}) and the film thicknesses were measured *in situ* by the vibrating quartz method. The thickness was also checked by a mechanical stylus profilemeter, in order to estimate the surface roughness of the thin films.

The structure of the films was checked by an X-ray goniometer. The morphology of the films was visualized by SEM.

The crystallographic state of the films was checked by transmission electron diffraction (TEM). In order to prepare the layers for TEM analysis, the NaCl crystals were dissolved in distilled water and the films were picked up with the usual copper grids. The TEM images were obtained using a "JEM 100 CX" electron microscope at a 100 kV acceleration voltage.

XPS analyses (carried out at University of Nantes, CNRS) were performed with a magnesium X-ray source (1253.6 eV) operating at 10 kV and 10 mA. The energy resolution was 1 eV at a pass energy of 50 eV. High-resolution scans with a good signal-to-noise ratio were obtained in the Se 3d and In 3d regions of the spectrum. The quantitative studies were based on the determination of the Se 3d and In $3d_{5/2}$ peak areas with 0.57 and 3.8 respectively, as sensitivity factors (the sensitivity factors of the spectrometer are given by the manufacturer, Leybold). The oxygen pollution in depth was studied by recording successive XPS spectra obtained after argon-ion etching for short

0022–2461

periods. Sputtering was accomplished at pressures of less than 5×10^{-4} Pa, 10 mA emission current and 5 kV beam energy using an ion gun. The Ar^+ ion beam was rastered over the entire sample surface. Quantitative analysis was also achieved by electron microprobe analysis.

The optical measurements were carried out at room temperature using a Cary spectrophotometer. The optical density, OD, was measured at wavelengths from 2–0.4 nm. The absorption coefficient, α, has been calculated from the measured transmission, $OD = \log(1/T)$, and from the averaged surface reflectivity, R, and the thickness, t, by $T = (1 - R)^2 \exp(-\alpha t)$. Because in the spectral regions of interest in this work the optical dispersion is small, the surface reflectivity has been taken to be effectively constant. It has been found [5] that R is about 0.3 between 2 and 0.4 nm for In_xSe_{100-x} amorphous thin films. Any errors incurred in the values of uncertainties induced by this technique are much less than the errors in the thickness measurements, which dominate the experimental errors. We have also calculated α from the transmission spectra of two samples of different thicknesses, t, because

$$\alpha = \frac{2.3(OD_2 - OD_1)}{t_2 - t_1} \quad (1)$$

However, we have used samples with quite small thickness differences because some authors [7, 17–19] have shown that the energy gap changed with the thickness of the sample. The energy gap is determined by extrapolating different plots of $\alpha h\nu = A(h\nu - Eg)^n$ to zero absorption; the value of n was chosen equal to 2 ($n = 2$), which is the most common law for amorphous semiconductors [11].

For electrical measurements, gold or aluminium electrodes were evaporated after the deposition of the thin films. The thermoelectric power (TEP) measurements have been performed at room temperature in order to determine the sign of the carriers. A system specially designed for highly resistive samples has been used [20].

3. Results

The composition and the crystalline state of the starting material are important due to the multiphase available in the In_xSe_{100-x} compounds.

We used powder of γIn_2Se_3 H (hexagonal), InSe R (rhombohedral) and In_4Se_3 as starting phase, as shown by X-ray diffraction spectra. Each composition was measured by microprobe analysis and by XPS. The results correspond to the phase expected (no deviation greater than 2 at % Se). The binding energies, found by XPS analysis, are in good agreement with those given elsewhere [21, 22].

Fig. 1 and Table I present the results of qualitative XPS analysis for In_xSe_{100-x} thin films. At the surface of the films, there is a carbon peak corresponding to pollution. This peak, which is situated at 284.8 eV, is used as reference for other binding energies [23]. So, a charge effect must be subtracted to the binding energies of the experimental curves shown in Fig. 1.

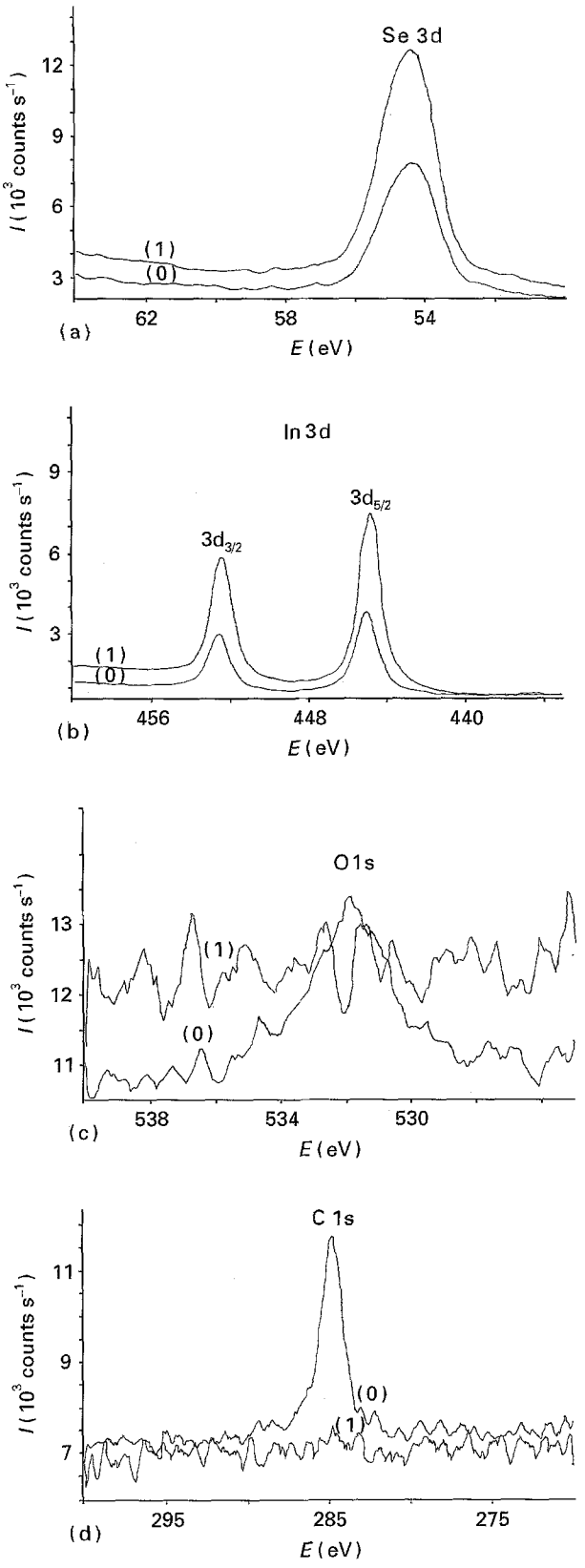

Figure 1 XPS spectra of (a) Se 3d, (b) In 3d, (c) O 1s, (d) C 1s, (0) before etching; (1) after 1 min etching. $In_{40}Se_{60}$ thin film.

A wide spectrum shows that there are no elements other than indium, selenium, carbon and oxygen in the layers. After 1 min etching, there is no carbon and oxygen left in the samples. The binding energy reference spectra were obtained from the literature [21, 22]. We can see that the In $3d_{5/2}$ peak is situated at 444.6 eV, while the Se 3d peak is situated at 54.2 eV.

TABLE I

Sample	Etching time (min)	Binding energy (eV)			Energy differences, ΔE (eV) between Se 3d and In $3d_{5/2}$	Composition (at %)			
		Se 3d	In $3d_{5/2}$	O1s		Se		In	
Antonangelli *et al.* [21]		54.2	444.6		390.4	50		50	
$In_{60}Se_{40}$	0	54.1	444.3	532	390.2	41	40[a]	59	60[a]
thin film	1	54.2	444.4	–	390.2	40		60	
$In_{50}Se_{50}$	0	54.5	444.9	531.7	390.4	48	47[a]	52	53[a]
thin film	1	54.4	444.8	–	390.4	47		53	
$In_{40}Se_{60}$	0	54.3	444.7	531.8	390.4	57	57[a]	43	43[a]
thin film	1	54.3	444.7	–	390.4	55		45	

[a] Microprobe analysis.

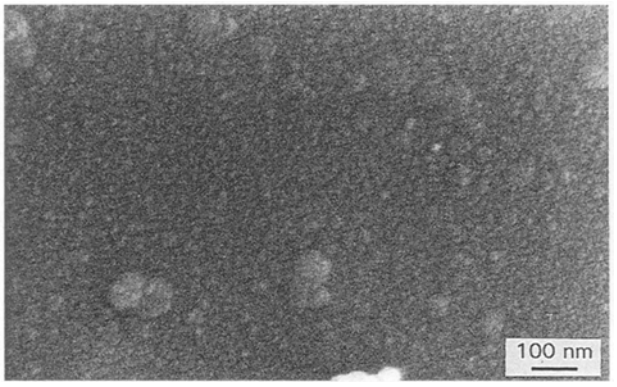

Figure 2 Typical scanning electron micrograph of an $In_{40}Se_{60}$ thin film.

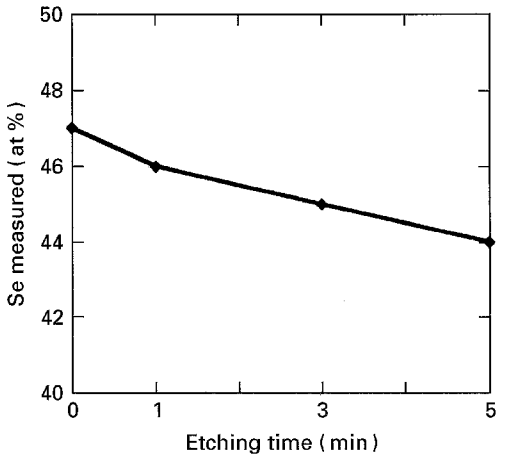

Figure 3 XPS elemental profile through the samples. (——) InSe reference powder, (◆) $In_{50}Se_{50}$ thin film of 400 nm.

Therefore, there is an energy difference between the In $3d_{5/2}$ and the Se 3d of 390.4 eV. The binding energies are very near to those obtained elsewhere [21, 22]. Owing to the energy resolution of our apparatus, the difference in binding energies between $In_{60}Se_{40}$, $In_{50}Se_{50}$ and $In_{40}Se_{60}$ thin films cannot be physically interpreted.

The surface of the films is very smooth, whatever the composition, as shown by SEM study (Fig. 2) and the stylus curve. When the SEM was used in the back-scattered mode, the surface of the film always appeared homogeneous, whatever the composition of the starting powder. The composition of the films has been measured by microprobe analysis and by XPS. The results (Fig. 2) confirm that the composition of the films does not differ from that of the starting powder. The homogeneity of the composition of the film was checked by microprobe. The variation from one point to another never exceeded 2 at % Se, which corresponds to the precision of the apparatus. It can be seen in Table I, that the results are in very good agreement with those obtained by microprobe analysis.

It has been shown by using reference powders, that the selenium was etched at a higher speed than indium. Therefore, we have used a reference powder in order to estimate the correction factors at different sputtering times, and then this has been used to calculate the corrected composition in depth for the corresponding film (Table I). As we can see in Fig. 3, the depth profiling of a layer was identical to that of the reference powder. We can conclude that the films have the expected composition, not only at the surface, but even in depth.

The amorphous state of the films was checked by X-ray diffraction and TEM. Because there is no peak visible on the XRD spectrum, it to supposed that the films are amorphous. But, as it can be seen in Fig. 4a and 5a, some inhomogeneities are present. There are small dark regions randomly scattered in a clear matrix. As $In_{50}Se_{50}$ and $In_{40}Se_{60}$ display the same structure, we have chosen to show only data for $In_{40}Se_{60}$ (Fig. 4a). The spots obtained from the dark areas are characteristic of microcrystallites randomly oriented (Figs 4b and 5b). Only diffuse rings are detected in the clear area, which confirms that the matrix is amorphous (Figs 4c and 5c). If we compare the micrographs of $In_{40}Se_{60}$ and $In_{60}Se_{40}$, we see that $In_{60}Se_{40}$ is less homogeneous than $In_{40}Se_{60}$, with a great number of dark areas, surrounded in $In_{60}Se_{40}$ by "less dark" domains.

Therefore, we can conclude that the films are amorphous with domains more or less crystallized, embedded in an amorphous matrix and that $In_{60}Se_{40}$ is far less homogeneous than $In_{50}Se_{50}$ and $In_{40}Se_{60}$.

After the physico-chemical characterizations of the films, some electrical and optical measurements were investigated.

As thickness seems to alter the electrical and optical properties of the amorphous InSe layers [7, 17–19], the following four measurements (α, σ, E_a, carrier type) were performed on samples of the same thickness (400 nm).

The values of the energy gap determined for $In_{60}Se_{40}$, $In_{50}Se_{50}$ and $In_{40}Se_{60}$ thin films are

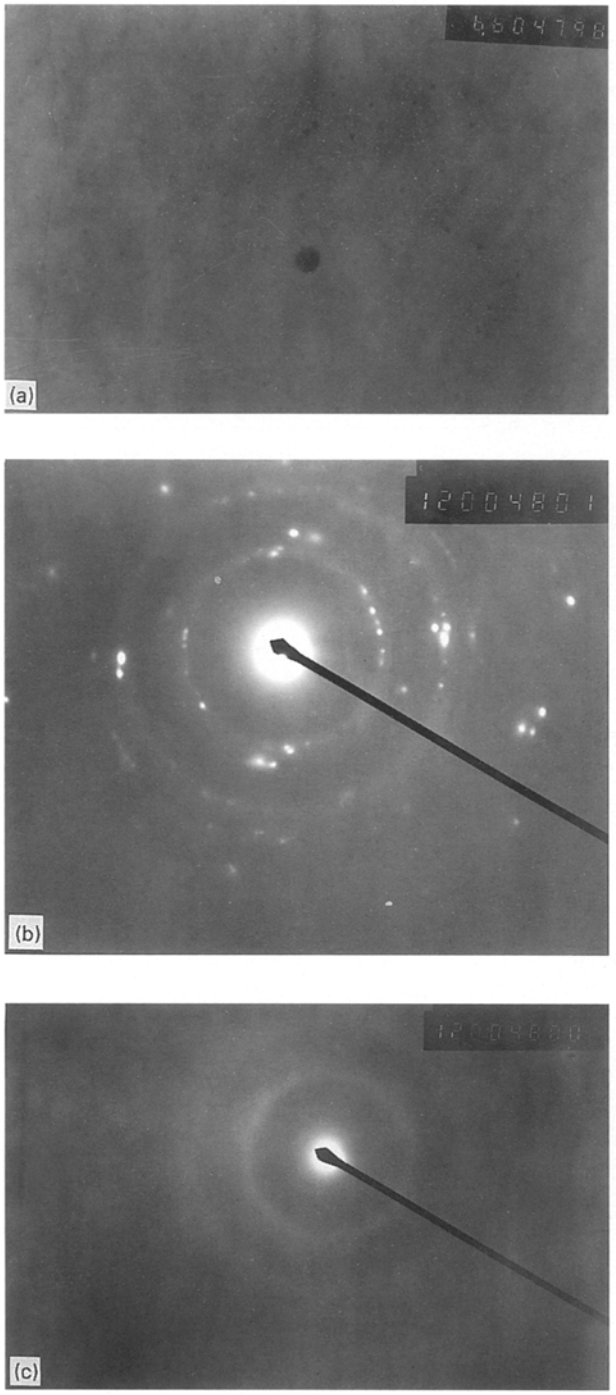

Figure 4 (a) Transmission electron micrograph of a $In_{40}Se_{60}$ thin film, (b) electron diffraction pattern of the dark area, (c) electron diffraction pattern of the clear area.

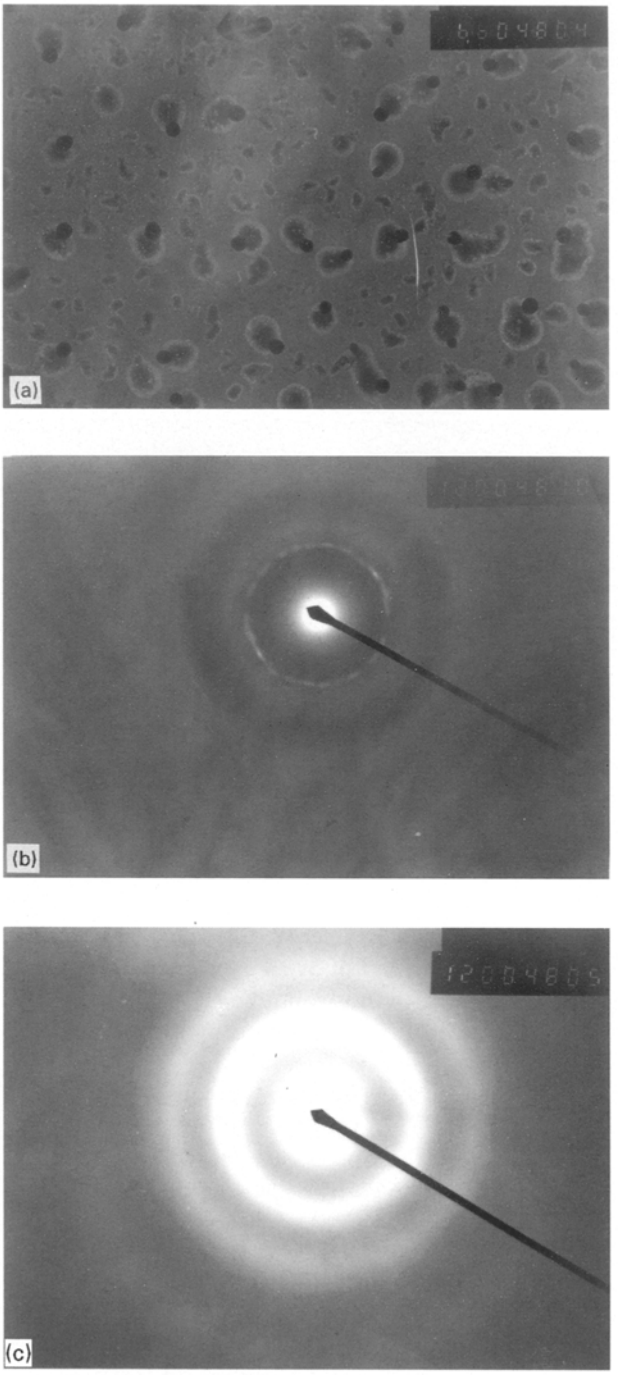

Figure 5 (a) Transmission electron micrograph of an $In_{60}Se_{40}$ thin film, (b) electron diffraction pattern of the dark area, (c) electron diffraction pattern of the clear area.

reported in Table II, and are in accordance with previous results [1, 5, 7, 12, 24]. It has been already found [12, 13, 25] that the value of the energy gap decreases with the decrease of selenium content (at %). The values of the conductivity for each film at room temperature are also reported in Table II. Our results are in good agreement with that found elsewhere [7, 12, 24]. Gold electrodes were used in order to obtain a good ohmic contact. The measurements, performed with aluminium electrodes, show very little difference from the present ones. A decrease of the conductivity with an increase in the selenium content is observed, as it was by other authors [12, 13, 26]. The activation energy for each sample has been deduced from the slope of the electrical conductivity variation $\ln \sigma = f(10^3/T)$, with T ranging from 240–440 K; the values are given in Table II.

The type of majority carriers has been deduced from TEP measurements. The results, reported in Table II, show that for compositions lying between 45 and 60 at % Se, a p-type conduction has been found, whereas for a selenium content less or equal to 40 at %, n-type behaviour has been observed. Gold and aluminium were both used for each kind of sample to prevent artefacts and the same results have been obtained.

TABLE II

	$In_{60}Se_{40}$	$In_{50}Se_{50}$	$In_{40}Se_{60}$
Gap (eV)	0.8	1.1	1.4
$\sigma_{\text{room temp}}$ ($\Omega^{-1}m^{-1}$)	1	3×10^{-3}	10^{-3}
Type	n	p	p
E_a (eV)	0.3	0.5	0.6

4. Discussion

It is well known that usually amorphous chalcogenides are p-type. This type comes from the creation of charged dangling bonds in this material. Mott and Davis [11] called these traps D^+ and D^-. The same authors have shown [11] that these traps pinned the Fermi level, E_f, near the middle of the gap. Kastner and Fritzsche [27, 28] showed that this theory can be improved, because some properties of the chalcogenides do not correspond to this model (too high densities of dangling bonds, origin of the negative effective correlation energy, U_{eff}, suspect, no explanations for a large negative U_{eff} in chalcogenides glasses, nor in tetrahedrally-bonded materials). Kastner and Fritzsche [27, 28] showed that these properties come from the creation of a valence alternative pair (VAP), called C_3^+ and C_1^- which pinned E_f near the middle of the gap, as in Mott and Davis' model.

In this work, we have found that $In_{40}Se_{60}$ and $In_{50}Se_{50}$ are effectively p-type, but that $In_{60}Se_{40}$ is n-type. This result will first be discussed on the basis of chemical bonds formed in the glasses.

Street and Lucovsky [29] have shown that the defect structure in chalcogenide alloys is complex because other types of defects, than C_3^+ and C_1^-, with similar properties are possible. For example, in pnictide-chalcogenide the positive defect may be either C_3^+ or P_4^+ (P represents pnictide) while both C_1^- and P_2^- are possible negative defects. They have also shown that, in all compounds, heteropolar bonding is energetically favoured, due to the effects of ionicity, and that the energy difference between heteropolar and homopolar bonding increases with the relative ionicities of the compounds. The electronegativity difference between indium and selenium is 0.7, which corresponds to the discussed value in this model.

Assuming that we have a large number of heteropolar bonding in our materials, we will now see the influence of the composition on the properties. Tohge *et al.* [30] studied chalcogenide glasses in the system Ge–Bi–Se. Starting from $Ge_{20}Se_{80}$, they showed that the simultaneous appearance of n-type conduction and of the abrupt decrease in resistivity near $Ge_{20}Bi_{10}Se_{70}$ composition can be related to the formation of fairly large number of Bi–Se bonds and the disappearance of Se–Se bonds. It has been shown elsewhere [11] that amorphous $In_{40}Se_{60}$ is composed of In–Se and Se–Se bonds, while in $In_{50}Se_{50}$ some In–In bonds begin to be present. So it can be guessed logically that $In_{60}Se_{40}$ contains a larger number of In–In bond than $In_{50}Se_{50}$. This hypothesis is corroborated by the fact that usually there is a preservation of the first coordination number of the corresponding crystal in amorphous semiconductors [11] and that there are many In–In bonds in the structure of crystalline In_4Se_3 [31].

Thus, in our case, we can see that the change in electrical and optical properties could be led by the formation of In–In bonds, and the disappearance of Se–Se bonds. It has been shown that usually an addition of 10%–15% doping agent can change the sign of carriers in amorphous chalcogenide. In our case, the percentage of indium that changes the properties has to be counted when the In–In bonds begin to appear, i.e. from at least 50 at % In. The change in carrier type accompanies a great increase in conductivity, a decrease in activation energy and in the optical gap, which is described here, as has been encountered by other authors [13, 29, 32–34]. Therefore, this result seems to be a classical one for doped chalcogenide alloys. But, even though Kumar *et al.* [32] and Tohge *et al.* [30] have studied the same compounds and have, moreover, obtained the same transition from p- to n-type by addition of bismuth, they have not interpreted this phenomenon in the same way: Tohge *et al.* [30] talk of bismuth's negative charge being compensated by the positive charge on the selenium atom, the presence of these new charged impurities tending to unpin the Fermi energy. Kumar *et al.* [32], on the other hand, talks of bismuth being positively charged. Negatively charged compensating defects are created (in order to conserve charge) which are chalocogen based, i.e. C_1^-. The law of mass action will ensure that positively charged chalcogen defects C_3^+ will be suppressed, thereby allowing the Fermi level to move towards the conduction band edge away from the position near mid-gap where it is normally pinned by the action of positive and negative defects. As a matter of fact, the electron concentration is increased, and an increase of the conductivity both with a drop of the activation energy is predicted. For our system owing to its lower electronic affinity, we can imagine that indium creates positive defects compensated by a suppression of chalcogen defects C_3^+, due to the electron issued from the In^+ defect. An argument for indium being the factor responsible of the change of the conduction type is its capacity to be a donor in some In–Se systems [35–38].

Anyway, this qualitative interpretation cannot be considered the only one for lack of further evidence. Moreover, the inhomogeneity domains visualized by TEM, and their growing size when the indium percentage increases has not been discussed above.

Many semiconducting films contain microscopic heterogeneities which significantly affect their electrical properties [39]. Direct observation of the microstructure is, in general, difficult, in many cases. They do not exhibit sufficient contrast for SEM observation. On the contrary, the existence of the microstructures must be inferred in a statistical sense (Maxwell–Garnett, Bruggeman). The approximations used are called effective medium approximations (EMAs) [39]. The Bruggeman EMA shows a percolation threshold low conductivity–high conductivity for an addition of a minimum amount of conductor of about 30%. Experimental results have shown that 15%–20%

concentration range is sufficient because at the percolation threshold filamentary rather than spherical regions become important leading to a lower threshold. A similar model has been used by Tichy *et al.* [33]. Hogg *et al.* [31] has shown that, in the In–Se system, indium tends to segregate when it is added in too great quantities. Therefore, indium clusters could exist, embedded in the amorphous matrix.

On the other hand, the transition from a poor conductive p-type to a conductive n-type behaviour can start at a certain critical concentration (percolation threshold) of the medium with n-type conductivity. We suppose that in the studied glasses such media could be InSe, In_2Se_3, In_4Se_3 submicroscopic entities (most probably clusters) embedded in a glassy matrix. We note that InSe, In_2Se_3 and In_4Se_3 are all n-type semiconductors [4, 40]. These areas are what we have called "dark areas" in the TEM results. They effectively exist in $In_{40}Se_{60}$, $In_{50}Se_{50}$ and $In_{60}Se_{40}$ but we can imagine that they are not linked for the two firsts by piles of indium, contrarily to the third one. As we can see on the transmission electron micrographs, the area of the inhomogeneities is larger in $In_{60}Se_{40}$, which is in good agreement with the hypothesis of percolation in this material. Thus, in $In_{40}Se_{60}$ and $In_{50}Se_{50}$, we can observe the usual carrier type for amorphous chalcogenide (p-type), as well as a low conductivity and a high activation energy corresponding to a Fermi-level pinned near the mid-gap. On the other hand, $In_{60}Se_{40}$, which has overreached what can be called percolation threshold, has a n-type conductivity (as the crystalline structure), a higher conductivity ($1\ \Omega^{-1}\,m^{-1}$) and a low activation energy which can be attributed to the microcrystalline structure. Nevertheless, the value of the conductivity is not that expected for the bulk crystalline material because it is a filamentary process.

The percolation theory was used by Tichy *et al.* [33] to explain the change of carrier type for Ge–Bi–Se system (the same system as Kumar *et al.* [32] and Tohge *et al.* [30]), which shows the difficulty in interpreting the results.

Concerning the conduction type, as mentioned in Section 1, in the case of the In–Se system: the experimental results themselves are different from paper to paper. Some papers insist that n-type amorphous films have been obtained in the In–Se system and some others, for the same composition, do not. This discrepancy in the experimental results cannot be solved without a discussion of the explanations why the n-type conduction is obtained in some amorphous films.

Between the two explanations proposed above, the former one is directly related to the composition of the layer because the change in carrier type is directly attributed to the increase of the indium percentage. The latter one is only indirectly bonded to the composition of the layer because for a given selenium percentage the morphology, size and the number of microscopic heterogeneities depends strongly on the deposition process. Of course the composition of the initial powder will be one of the parameters influencing the morphology of the layers but, the starting material, the vacuum, the evaporation source, the deposition technique, the evaporation rate, the substrate temperature, etc., will be also very important. Therefore in the light of this discussion we can think that the latter explanation is more able to explain the discrepancy of the experimental results.

The evolution of the optical gap, for his part, can be interpreted in the same way, whatever is the change of the conduction type interpretation. Even in the case of conduction by a filamentary process, the volume ratio of the crystalline phase on the amorphous phase is too small to create significant alteration of the results of the optical measurements. These measurements are indeed based on a beam going through the whole sample; it can be noticed that the same reasoning can be applied to the XPS analysis as well as the microprobe analysis, which explains why we do not see much difference, whatever the composition (the volume of the amorphous matrix is always much greater than that of the crystalline structure). Therefore, the evolution for the optical gap is interpreted by the evolution of the chemical bonds length in the amorphous matrix. Mott and Davis [11] have shown that the In–Se and Se–Se bonds length increases when the composition varies from $In_{40}Se_{60}$ to $In_{50}Se_{50}$ and we can imagine that this evolution continues from $In_{50}Se_{50}$ to $In_{60}Se_{40}$, as is the case in the crystalline structures [11, 31]. The evolution of the optical gap, which decreases from $In_{40}Se_{60}$ to $In_{60}Se_{40}$, is then simply interpreted by the increase of the chemical bonds length from $In_{40}Se_{60}$ to $In_{60}Se_{40}$.

5. Conclusion

A change in carrier type from p- to n-type, as well as an increase of the conductivity, a decrease in the activation energy and in the optical gap, has been observed for In_xSe_{100-x} alloys when x varies from 40–65. These results have been interpreted, on the one hand, by a theory based on the relative percentage evolution of the In–In and Se–Se chemical bonds and, on the other hand, by a percolation theory due to microcystalline structures and indium filaments.

We have shown that X-ray diffraction spectra and not sufficient to determine whether or not the thin film contains microcystalline structures, and then to determine the origin of the majority carriers' type. The choice of the x-variation interpretation for In_xSe_{100-x} amorphous thin-film properties is made difficult by both the mixture of the amorphous and microcrystalline structure and the nature of the new defects introduced when the In–In bond percentage increases. A high-resolution transmission electron microscopy (HRTEM) analysis can be envisaged to discriminate whether the chemical bonds or the percolation theory is the right one.

Acknowledgements

The authors thank Mr G. Michel, and A. Barreau, for performing measurements, Mrs C. Vadcard and C. Thébaud, for their helpful work, and Mr J.Y. Masson for helpful discussions.

References

1. K. ANDO and A. KATSUI, *Thin Solid Films* **76** (1981) 141.
2. T. MATSUSHITA, A. SUZUKI, M. OKUDA and T. SAKAI, *Jpn. J. Appl. Phys. Suppl.* **19/2** (1980) 123.
3. M. DIGIULIO, G. MICOCCI, A. RIZZO and R. TEPORE, *J. Appl. Phys.* **54** (1983) 5839.
4. A. SEGURA, J. P. GUESDON and J.M. BESSON, A. CHEVY, *ibid.* **54** (1983) 876.
5. M. DIGIULIO, G. MICOCCI, R. RELLA. P. SICILIANO and A. TEPORE, *Thin Solid Films* **148** (1987) 273.
6. Y. HASEGAWA and Y. ABE, *Phys. Status Solidi A* **70** (1982) 615.
7. M. A. KENAWY, A. F. EL-SHAZLY, M. A. AFIFI, H. A. ZAYED and H. A. EL-ZAHID, *Thin Solid Films* **200** (1991) 203.
8. S. P. GRINDLE, *J. Appl. Phys. (USA)* **51** (1980) 5464.
9. F. S. JIANG, L. HOU, S. and F.X. GAN, in "Proc. SPIE Optical Data Storage Topical Meeting", Vol. 1078 (International Society Optical Engineers, USA, 1989) 165.
10. K. UTSUMI, V. GOTO, I. TSUGAWA, T. YUASA, N. KOSHINO and S. OGAWA, in SPIE, Optical Storage Technology and Application, Vol. 899 (International Society Optical Engineers, USA, 1988) p. 196.
11. N. F. MOTT and E. A. DAVIS, "Electronic Process in Non-Crystalline Materials", 2nd Edn (Clarendon Press, Oxford 1979).
12. A. B. ONYS' KIV, YU M. ORISHCHIN, U. P. SAVCHIN, I. M. STAKHIRA, I. M. FETSYUKH, *Sov. Phys. Semicond.* **24** (1990) 264.
13. I. WATANABE and T. YAMAMOTO, *Jpn J. Appl. Phys.* **24** (1985) 1282.
14. H. NAITO, M. OKUDA, T. MATSUSHITA and T. NAKAU, *Jpn J. Appl. Phys.* **19** (1980) L513.
15. S. RAMCHANDAR RAO, M. NAGABHOOSHANAM and V. HARI BABU, *Cryst. Res. Technol.* **25** (1990) 55.
16. T. MATSUSHITA, T. T. NANG, M. OKUDA, A. SUZUKI and S. YOKOTA, *Jpn J. Appl. Phys.* **15** (1976) 901.
17. S. K. BISWAS, S. CHAUDHURI and A. CHOUDHURY, *Phys. Status. Solidi (a)* **105** (1988) 467.
18. D. V. KRISHNA SASTRY and P. JAYARAMA REDDY, *Thin Solid Films* **105** (1983) 139.
19. J. SHIGETOMI, H. OHKUBO and T. IKARI. *J. Appl. Phys.* **66** (1989) 215.
20. J. C. BERNÈDE, G. SAFOULA, A. AMEZIANE and P. BURGAUD, *Phys. Status Solidi (a)* **11** (1988) 521.
21. F. ANTONANGELLI, M. PIACENTINI, A. BALZAROTTI, V. GRASSO, R. GIRLANDA and E. DONI, *Il Nuovo Cimento* **51 B**(1) (1979) 181.
22. C. D. WAGNER, W. M. RIGGS, M. E. DAVIS, S. F. MOULDER and G. E. MUILENBERG, "Handbook of X-ray Photoelectron Spectroscopy CD" (Perkin-Elmer, Eden Prairie, MN, 1979).
23. C. CARDINAUD, G. TURBAN, B. CROS and M. RIBES, *Thin Solid Films* **205** (1991).
24. R. ROUSINA, G. K. SHIVAKUMAR and G. H. YOUSEFI, *Vacuum* **41** (1990) 1451.
25. T. P. SHARMA, S. K. SHARMA, R. KUMAR and GARINA JAIN, *Ind. J. Pure Appl. Phys.* **28** (1990) 486.
26. A. KUMAR, M. M. MALIK, M. ZULFEQUAR, A. KUMAR and M. HUSAIN, *Solid State Commun.* **79** (1991) 699.
27. M. KASTNER, *J. Non-Cryst. Solids* **31** (1978) 223.
28. M. KASTNER and H. FRITZSCHE, *Philos. Mag.* B **37** (1978) 199.
29. R. A. STREET and G. LUCOVSKY, *Solid State Commun.* **31** (1979) 289.
30. N. TOHGE, T. MINANI, Y. YAMAMOTO and M. TANAKA, *J. Appl. Phys.* **51** (1980) 1048.
31. J. H. C. HOGG, H. H. SUTHERLAND and D. J. WILLIAMS, *Acta Crystallogr.* **B 29** (1973) 1590.
32. S. KUMAR, S. C. KASHYAP and K. L. CHOPRA, *Thin Solid Films* **217** (1992) 146.
33. L. TICHY, H. TICHA and A. TRISKA, *Solid State Commun.* **53** (1985) 399.
34. T. T. NANG, M. OKUDA, T. MATSUSHITA, S. YOKOTA and A. SUZUKI, *Jpn J. Appl. Phys.* **15** (1976) 849.
35. F. ABOU-ELFOTOUH, D. J. DUNLAVY and T. J. COUTTS, *Solar Cells* **27** (1987) 237.
36. S. M. WASIM, *ibid.* **16** (1986) 289.
37. J. A. THORNTON, T. C. LOMMASSON. H. TALIEH and B. H. TSENG, *ibid.* **24** (1988) 1.
38. A. ROCKETT, T. C. LOMMASSON, P. CAMPOS, L. C. YANG and H. TALIEN, *Thin Solid Films* **171** (1989) 109.
39. A. H. CLARK, *ibid.* **108** (1983) 285.
40. D. BIDJIN, S. POPOVIC and B. CELUSTKA *Phys. Status Solidi (a)* **6** (1971) 295.

Received 12 January
and accepted 22 June 1995